

Autores (p. o. de firma): E. Gimeno-García, V. Andreu & J.L. Rubio

Título: Spatial patterns of soil temperatures during experimental fires

Revista: Geoderma

Volumen: 118 Página inicial: 17 Página final: 38 Año: 2004

1 **Spatial patterns of soil temperatures during experimental fires**

2
3 E. Gimeno-García ^{*}, V. Andreu & J.L. Rubio

4 *Centro de Investigaciones sobre Desertificación- CIDE (CSIC, Universitat de València,*
5 *Generalitat Valenciana). Camí de la Marjal s/n, 46700-Albal, Valencia, Spain*

6 7 8 **Abstract**

9
10 The main objective of this paper is to assess the spatial patterns of temperature
11 distribution at the soil surface after a shrubland fire in a typical Mediterranean environment.
12 The study was carried out by making experimental fires at a permanent field station (La
13 Concordia, Valencia, Spain) in a typical Mediterranean forest slope. The set up consisted of
14 nine plots (20 m long by 4 m wide) with similar morphology, slope gradient, rock outcrops,
15 soil (Rendzic Leptosol) and vegetation cover (*Rhamno lycioidis-Quercetum cocciferae*
16 association). Two different fire severities were evaluated, high (F2) and moderate (F1),
17 created by the addition of limited amounts of biomass. To measure soil temperatures, two
18 complementary methods were used: thermocouples and thermosensitive paints. Results show
19 that peak temperatures on the soil surface measured by the two systems (higher than 600°C in
20 most cases) are quite similar and there are not statistically significant differences between
21 them. The mean values of soil surface temperatures measured with thermosensitive paints
22 were 240, 239 and 218°C for F1 plots and 418, 448 and 435°C for F2 plots. Half of the F1
23 plots surface showed temperature values between 170 and 235°C, and in the F2 plots these
24 values ranged between 322 and 543°C. Geostatistics were applied to analyze and describe the

* Corresponding author. Tel.: +34-96-1220540; fax: +34-96-1270967. *E-mail:* eugenia.gimeno@uv.es

25 spatial variation of soil temperatures at the soil surface. Results showed that there are two
26 dominant spatial patterns of temperature distribution (spherical and linear). The spherical
27 model varied approximately between 4 and 10 m, and its pattern is related mainly to the
28 natural biomass distribution and the time of flame persistence. In the second, the linear
29 pattern, the temperature rises from the lower part to the upper part of the plot and seems to be
30 controlled by the meteorology at the time of burning, mainly by the wind speed and wind
31 direction.

32 The spatial patterns of soil temperatures during the studied experimental fires affect
33 soil properties in different ways according to the fire severity. This fact could contribute to
34 change the spatial dynamics of soil nutrients that will play an important role in the recovery of
35 the burned vegetation.

36

37 *Keywords:* Experimental fire, Mediterranean, spatial patterns, soil properties, soil temperature

38

39

40 **1. Introduction**

41

42 One of the most important perturbations of Mediterranean forest ecosystems is fire,
43 both by natural or anthropogenic causes. Fire produces a wide spectrum of responses in the
44 affected ecosystems that depends on the interaction of many factors, including fire severity,
45 fire intensity, duration of temperatures, fuel loading, degree of combustion, vegetation type,
46 climate, slope, topography, soil characteristics, time since last fire, and area burned (Neary et
47 al, 1999).

48 Fire severity is a qualitative measure of the effects of fire on site resources (Hartford
49 and Frandsen, 1992; Ryan and Noste, 1983). As a physico-chemical process, fire produces a

50 spectrum of effects that depends on the interaction of energy released, duration, fuel loading
51 and combustion, vegetation type, climate, topography, soil and area burned (Robichaud et al.,
52 2000). Fire intensity is an integral part of fire severity, and it refers to the rate at which a fire
53 produces thermal energy (DeBano et al., 1998). Intensity is measured in terms of temperature
54 and heat yield. Surface soil temperatures can be as a little as 50 °C to as high as 1500 °C. Heat
55 yields per unit area can range from 1088.57 KJ m⁻² to greater than 41868 KJ m⁻², depending
56 on the fuel type (Pyne et al., 1996). The most damaging component of fire severity to soil,
57 and hence to ecosystem stability, is its duration (Robichaud et al., 2000).

58 Fire severity cannot be expressed as a single quantitative measure that relates to
59 resource impact. Relative magnitudes of fire severity, expressed in terms of the post-fire
60 appearance of litter and soil (Ryan and Noste, 1983), are widely used criteria for placing fire
61 severity into broadly defined, discrete classes, ranging from low to high. However, some
62 aspects of fire severity can be quantified. Because of fire effect on soil properties mainly
63 depends on peak temperatures and their duration, several researchers have used mainly these
64 two quantitative variables to evaluate the impact of fires on soil properties.

65 It is difficult to characterize fire severity within individual fires or between different
66 fires owing to the intrinsic experimental difficulties, the great variability of combustion
67 processes and soil conditions. During experimental fires, soil temperatures and their duration
68 are best measured by means of thermocouples, which allow the continuous recording of
69 temperatures at a given place. Nevertheless, obtaining detailed information on the spatial
70 variability of those parameters using thermocouples is expensive because of the need of using
71 a huge number of them. Thermosensitive paints are an alternative method for obtaining the
72 spatial variability of soil temperatures during experimental fires. Although these devices only
73 provided the maximum temperature reached at a given place, they have proved to be valuable
74 in understanding the response of soils and organisms to spatial changes of temperature during

75 a fire (DeBano and Conrad, 1978; Moreno and Oechel, 1992; Marion et al., 1991; Moreno
76 and Oechel, 1994; Pérez and Moreno, 1998).

77 To assess the spatial variability of soil temperature values reached during a fire,
78 mathematical descriptors –quantitative models- of that variation have been developed. Their
79 applicability requires a different approach from that of classical statistics. It is embodied in
80 the Regionalized Variable Theory, the practical application of which is Geostatistics (Webster
81 and Oliver, 1990).

82 This paper is focused on the evaluation of the temperatures in the soil surface during
83 shrub fires, through their measurement by means of thermosensitive paints, and to identify the
84 spatial patterns of soil temperature distribution. The short-term interactions between fire
85 severity and the immediate changes in some soil properties have also been studied.

86

87

88 **2. Materials and methods**

89

90 *2.1. Experimental site*

91

92 The study area of ‘La Concordia’ (latitude 39°45’ N and longitude 0°43’W) is located
93 in the municipality of Liria (Valencia, Spain), 50 km NW of Valencia city, on land ceded by
94 the Forestry Services of the Valencia Government (Generalitat Valenciana). The selected
95 hillside, South-South East facing, is 575 m above the sea level and has a 30% slope. The
96 vegetation cover is a sclerophyllous shrub regenerated after a previous wildfire occurred in
97 1978. The dominant vegetation type belongs to the *Rhamno lycioidis-Quercetum cocciferae*
98 association, which is typical of semi-arid Mediterranean areas. Climatically the area belongs
99 to the dry ombroclimate of the lower mesomediterranean belt, according to Thornthwaite’s

100 classification (Rivas-Martínez, 1981). The average annual precipitation is around 400 mm
101 with two maxima, autumn and spring, and a dry period from June to September. Mean
102 monthly temperatures range from 13.3°C in January to 25.8°C in August. The soil is a
103 Rendzic Leptosol (FAO-UNESCO, 1988) developed on Jurassic limestone, and shows a
104 variable depth, always less than 40 cm, good drainage, a sandy-loam texture and an alkaline
105 pH (7.4). Soil physical and chemical properties are shown in Table 1.

106 The experimental set-up consists of nine plots, 20 m long by 4 m wide each, with
107 similar morphology, slope gradient, rock outcrops, soil and vegetation cover. The location of
108 each plot was made after intensive surveys of vegetation, soil and morphology patterns, based
109 on an across-slope transect every 2 m.

110

111 *2.2. Natural biomass quantification*

112

113 Composition and spatial distribution of the vegetation in each plot were determined by
114 identifying the species, counting their individuals and measuring their size (height, maximum
115 and minimum diameter in cm), as well as the percentage of soil covered by plants on a 1m x
116 1m grid basis. This information was used to map dry biomass and vegetation cover present in
117 each square meter and to calculate the mean dry biomass present in the plots.

118 Dry biomass was estimated by using a non-destructive methodology similar to those
119 proposed by Etiene (1989), Etiene and Legrand (1994) and Martínez-Fernández et al. (1991).
120 Different algorithms and equations based on this methodology, which related dimensions and
121 dry weight for the dominant species, were used to calculate the dry weight of each species,
122 where the independent variable was the weight and the dependent variable was the volume. A
123 known geometrical form was assigned to each species based on visual observations of their
124 architecture (for example, a truncated and inverted cone for *Rosmarinus officinalis* and a

125 cylinder for *Ulex parviflorus*). To quantify the dry weight, several individuals of the dominant
126 species (8 individuals of *Rosmarinus officinalis*, 8 individuals of *Ulex parviflorus*, 3
127 individuals of *Stipa tenacissima*, 2 individuals of *Quercus coccifera*) were selected in the
128 surrounding area and their height and diameters measured. Afterwards, they were cut and the
129 samples were taken to the laboratory, where biomass was weighed and placed in an oven 48 h
130 at 55°C and, finally volumes and dry weights were linearly regressed. Under the three species
131 that cover the highest percentage of soil surface (*Ulex parviflorus*, *Rosmarinus officinalis* and
132 *Quercus coccifera*), 9 litter samples on a grid of 25 cm x 25 cm were collected and the
133 biomass was also directly measured.

134

135 2.3. Experimental fire treatments

136

137 Two experimental fire treatments were applied to reach different fire severities. The
138 assignment of fire treatments to each plot was random. The first treatment (F1) consisted of
139 the addition of biomass up to 2 kg m⁻² to three plots. In the second treatment (F2) up to 4 kg
140 m⁻² was added to other three plots. The added biomass was obtained from the surrounding
141 shrub vegetation and it was spread uniformly on the plots. This creates fuel continuity inside
142 each plot by covering the areas of bare soil. The third set of three plots was used as a control.

143 Experimental fires were carried out under field conditions on 20 and 21 June 1995.
144 Climatic parameters were monitored by a logging system of sensors placed close to the plots.
145 Video records of the fire progression were taken to follow and to study the fire behaviour in
146 each plot. Height sticks, 2-m long, were placed along both sides of the plots at 2-m interval,
147 as reference points for photography and video for following the speed of the fire progression.
148 Moreover, rate of spread of the fire front was measured by direct timing of the front passing
149 these markers.

150 To measure soil temperatures, two complementary methods were used: thermocouples
151 and thermosensitive paints. The first system allows to obtain information on the peak
152 temperatures and to know the duration that the soil system is exposed to high temperatures,
153 whereas the second system allows monitoring of the spatial distribution of peak temperatures
154 on soil surface.

155 To obtain the continuous temperature-time curves on the soil surface as well as to
156 measure the peak temperatures and their duration, thermocouples were used. Six
157 thermocouples (type K Inconel 600 insulated) per plot were installed at ground level along
158 parallel lines running downslope and separated from one another by 3 m. From these
159 measurements direct estimates were made of the time that temperature exceeded 100 °C. This
160 value was chosen because it seems to be at which the most significant changes on soil
161 properties begin, starting with water evaporation.

162 To obtain the spatial distribution of temperatures on soil surface a set of
163 thermosensitive paints were used (Omega Stick Crayons®) ranging between 100°C and
164 677°C, at increments of approximately 25°C. They liquefy according to the temperature
165 reached. A total of 24 paints were applied on iron rods (250 mm long x 14 mm wide x 3 mm
166 high). They were covered with another identical rod, but unpainted, which protect the paints
167 from the possible disturbance produced by ashes and flames. The system was tied with two
168 pieces of wire. Just before the experimental fire, one iron rod per square metre was placed (a
169 total of 80 iron rods per plot) with the painted side in contact with soil. Immediately after the
170 passage of fire, the iron rods were collected and read. In each burned plot, there were six
171 points where thermocouples and thermosensitive paints were placed close together. Thus, a
172 comparison between temperature measurements through both methods was made.

173

174 2.4. Soil analysis

175

176 Immediately before the fires, 36 soil samples (four per plot) at 0-5 cm depth were
177 taken. Litter was removed prior to sampling. The soil samples were air-dried, sieved to
178 remove material with diameter >2mm, and stored in airtight plastic boxes until analysis.

179 The soil parameters measured and the analytical methods used were: organic matter
180 content by oxidation with potassium dichromate (Jackson, 1958); soil texture by pipette
181 method (Ministerio de Agricultura, Pesca y Alimentación, 1986); soil bulk density (Blake and
182 Hartage, 1986a), particle density (Blake and Hartage, 1986b); water retention capacity at field
183 moisture level (Demolon, 1965); soil moisture content by the gravimetric method; aggregate
184 stability by Hénin and Feodoroff method modified by Primo and Carrasco (1973); electric
185 conductivity and pH (Richards, 1954); total carbonates (Douchafour, 1965); total nitrogen
186 determined by micro-Kjeldahl automatic analyser using the Bremner method (Black et al.,
187 1965); mineral nitrogen determined by steam distillation by micro-Kjeldahl automatic
188 analyser using the Bremner method (Black et al., 1965); available phosphorus determined by
189 colorimetry according to method of Olsen and Dean (Black et al., 1965); and cation exchange
190 capacity determined according to the method of Bower et al. (1952).

191 Volumetric heat capacity was estimated using the equation proposed by Hillel (1980):

192
$$C_v = f_m C_m + f_o C_o + f_w C_w$$

193 where: C_v is the volumetric heat capacity of the soil ($\text{KJ m}^{-3} \text{K}^{-1}$), f_m represents the volume
194 fraction of mineral soil (1.49 in the present case), C_m is the volumetric heat capacity of the
195 mineral fractions ($2.0 \text{ KJ m}^{-3} \text{K}^{-1}$), f_o denotes the volume fraction of organic matter (0.172 in
196 our case), C_o is the volumetric heat capacity of the organic fraction ($2.51 \text{ KJ m}^{-3} \text{K}^{-1}$), f_w
197 represents water fraction in the soil, and C_w is the volumetric heat capacity of water (4.18 KJ
198 $\text{m}^{-3} \text{K}^{-1}$).

199 C_v was calculated for three different soil water conditions: dry soil ($f_w = 0$), soil water
200 content at the time of sampling, and for soil field capacity. Calculations were made before and
201 after fire and they take into account the first 5 cm of soil.

202

203 2.5. Statistical Analysis

204

205 Analysis of variance (ANOVA) was made to test significant differences between the
206 two fire treatments. Statistical analysis of the temperature data was done in two stages: (1)
207 description of their distribution using traditional statistics and with the median and
208 interquartile range, which are less influenced by skewed distributions; (2) definition of semi-
209 variograms, in which the differences in nugget and total semivariance and range were
210 examined for the variable temperature.

211 The semi-variance function $\gamma(h)$ is equal to half the expected squared difference
212 between values at locations separated by a given lag and it is used to express spatial variations
213 (Journel and Huijbergts, 1978). The semivariance calculation, semivariogram function model
214 fitting and kriging were performed using the GS+ software (Gamma Design Inc.; Plainwell,
215 MI). On each plot, 80 observations were taken at a regular interval $z(i)$, where $i=1, 2, \dots, n$,
216 semi-variances were calculated using the equation:

$$217 \quad \gamma(h) = \frac{1}{2N(h)} \sum_{i=1}^{N(h)} [z(x_i) - z(x_{i+h})]^2$$

218 where $\gamma(h)$ is the sample semivariance; $N(h)$ is the number of pairs of data points separated by
219 the distance h , and $z(x_i)$ and $z(x_{i+h})$ are the values of the temperature at locations separated by
220 the vector h . This is known as the lag. We used a lag interval of 1 m, which resulted in a
221 minimum of nine samples in the smallest lag interval (0-1 m) and a maximum of 700 pairs in
222 the 1-2 m interval. Our analysis extends to a lag of 11.5 m, 2/3 of the maximum lag interval.

223 The isotropic semivariograms were fitted by weighted least-squares analysis to several
224 models. The linear, linear/sill, spherical, exponential and gaussian models were explored as
225 models to fit the semivariogram functions for the soil temperature.

226 Punctual kriging, which is an exact interpolator (Delhomme, 1978), was used to
227 estimate values of soil surface temperature for unsampled locations. To show the spatial
228 distribution of soil temperatures throughout the plots, estimates were generated using the
229 punctual kriging technique at 0.1-m intervals. The 8 nearest neighbour values to an estimation
230 point with a maximum radius of 19 m were used to obtain kriged estimation. The jack-knifing
231 procedure was used to test adequacy of the selected semi-variance models plus kriging
232 parameters (search radius, etc). Finally, the results of the kriging were displayed as a contour
233 map.

234

235

236 **3. Results and discussion**

237

238 *3.1. Natural biomass distribution*

239

240 Inside the plots, marked differences in natural fuel distribution were observed. The
241 mean values of plant and litter biomass obtained as well as the percentage of soil cover is
242 reflected in Table 1. The most abundant species were *Rosmarinus officinalis*, *Ulex parviflorus*
243 and *Globularia alypum*, which represented between 60% (plot 8) and 90% (plot 2) of the
244 number of the individuals. Table 2 shows the distribution frequencies of the main species in
245 La Concordia plots. In most plots, approximately the 50% of their surface showed a quantity
246 of biomass \leq to 0.5 kg m^{-2} (Figure 1).

247 It is important to note that despite of the homogeneous addition of biomass in each fire
248 treatment, neither the compactness of the added vegetation nor their moisture content were
249 equal to the standing biomass and litter present in each plot. Thus, differences in the spatial
250 patterns of soil temperatures could be expected. Moreover, as it can be observed in Section
251 3.3., the distribution of bare soil and vegetation in a patchy shrub mosaic, typical of the
252 Mediterranean semiarid vegetation cover pattern, play an important role during the fire spread
253 by increasing variability of fire intensity and soil temperature.

254

255 *3.2. Behaviour of the experimental fires*

256

257 The meteorological conditions at the time of burning are reflected in Table 3. It can be
258 seen that the experimental fires were carried out under similar climatic conditions,
259 considering air temperature, relative humidity and wind speed. The fire front progressed
260 rapidly upslope (in less than 2 min all the plots were covered by flames), and their behaviour
261 were quite uniform in all the plots, except in plot 6 that suffers repeated changes in wind
262 direction, but not affected the general pattern of fire spread. In all cases, the fire progression
263 from their start to the lower middle part of the plots was faster in the centre of fire front than
264 in their flanks. When the lower half part of the plots length were passed the fire front
265 progressed more uniformly.

266 The description of fire behaviour in each plot was made analysing the video recording
267 and through the observations make during the fire performance. Figures 2 and 3 show the
268 schematic representation of fire progression. Note that the time data indicated in each figure
269 comes from the visual and video estimation of flame persistence. The combustion processes
270 of biomass have a longer duration.

271

272 *3.3. Spatial variation of soil temperatures*

273

274 Table 4 shows the comparison between the maximum temperatures measured with
275 thermocouples and thermosensitive paints. Results show that peak temperatures on the soil
276 surface, measured by the two systems, are quite similar and there are not statistically
277 significant differences. Thermocouples measurements in plot 7 failed, and they are not
278 included in the statistical analysis. The significant differences between temperature values in
279 the burned plots correspond to the different fire treatments (F1 and F2). The mean duration of
280 soil temperatures greater than 100°C was 17.6 minutes for the F1 treatment, and 36.3 minutes
281 for the F2 treatment.

282 From the thermosensitive paints, data of mean and median were used as the primary
283 estimates of the central tendency, and the standard deviation, CV and interquartile range were
284 used as estimates of variability (Table 5). Despite the skewness of the distributions, the mean
285 and median values for soil temperature were similar, with the medians having smaller values
286 than the means in most cases (Table 5).

287 Results obtained show that 50% of temperature values in F1 plots were between 170
288 and 235 °C. These values ranged between 322 and 543 °C in the F2 plots. The mean values
289 obtained of soil surface temperatures measured with the thermosensitive paints were 240, 239
290 and 218 °C for the three F1 plots, whereas for the F2 plots these values were 418, 448 and 435
291 °C (Table 5). ANOVA shows that there are statistically significant differences between the
292 two fire treatments.

293 If the mean values of soil temperature are taken into account, results show the more
294 biomass the higher temperatures at soil surface. Mean temperature values for F2 plots are
295 much greater (~200°C) than for F1 plots. However, analysing the increase of temperatures
296 related to the amount of biomass present in the plots, it can be seen that there is not a linear

297 relation between these variables (Figure 4). Nevertheless, in most cases, there are significant
298 linear correlations between the increase in temperatures and the distance covered by the fire
299 line (Figure 5), which means that as the flame front raised upslope the soil surface
300 temperatures increased.

301 Fire behaviour is probabilistic and irregular rather than uniform; variable in intensity
302 as well as in size (Pyne et al., 1996). When wind or slope acts on a fire, flames can be bent
303 down and the fire adopts a direction in which concentrates its convective flow, then, more of
304 the released heat can be directed onto new fuel. Rather than dissipating its heat in all
305 directions, the heat is focused (Pyne et al., 1996). This is the pattern that occurs in our
306 experimental circumstances.

307 The soil temperature showed differences in their spatial dependence, as determined by
308 their semivariances. Semivariogram models and model parameters for the soil surface
309 temperature are shown in Table 6. In our case, the spherical and linear are the best-fit models.
310 There is no relationship between fire treatment and semivariogram best-fit model. Jack-
311 knifing procedures indicated that the model parameters plus kriging parameters are acceptable
312 for all the semi-variogram models fitted to each plot. The resulting statistics from the jack-
313 knifing analysis show that, in all cases, the mean error is close to 0 (oscillate between 0.02
314 and 0.05) and the variance of the standardised residuals is close to 1 (between 0.7 and 1.03)
315 (Table 6).

316 Spherical models were defined for soil temperatures measured on plots 1, 4 and 7. For
317 plot 1 the best-fit model parameters indicated that the exponential model is best. This
318 semivariogram approach its sill asymptotically. Strictly it has no range. For practical purposes
319 their effective range is taken as the lag distances at which reach 0.95% of the sill variance
320 (Webster and Olivier, 1990). In a few cases, where differences in r^2 were <0.05 between the
321 spherical and alternative models, the spherical model was used to allow direct comparison of

322 the nugget, sill and range values among soil temperature (Cambardella et al., 1994). In the
323 case of plot 1, the exponential model generates estimates of nugget and total semivariance
324 that are similar to the spherical model, and the difference between the r^2 from each model was
325 only 0.017.

326 The shape of the semivariogram for plot 1 (Figure 6a) suggests that some
327 autocorrelation occurs among points <3.8 m apart, with the strongest autocorrelation among
328 points separated by <1m interval. Progressively, less correlation occurs among points >2 m
329 distant, such that at 3.8-m intervals, the variance attributable to autocorrelation becomes
330 approximately equal to the population variance. Thus, sample points separated by >3.8 m
331 appears independents of one another.

332 The same trend is observed for temperature data in plots 4 and 7 (Figures 6b and 7c),
333 although the range values increases. The range in plot 4 is 9.28 m, which indicates that the
334 spatial pattern vary each 9.8 m, and the points <9.8 m apart have more similar temperature
335 values. In plot 7, the range value is 10.3 m. In these cases the range values provides an
336 estimation of areas that have reached similar temperatures. These patches roughly coincide
337 with the patchy distribution of pre-fire natural vegetation and litter.

338 Soil temperatures in plots 2 and 8 are described by a linear semivariogram (Table 6,
339 Figures 7a and 6c), which suggests that, as the spatial distance between two measured points
340 increases, the difference between them will also increases.

341 If the linear model has a slope close to zero, as occurs in plot 6 (Figure 7b), then the
342 total variance is equal to the nugget variance and, in this case, the variable is described as
343 spatially independent and completely random at the scale of the measurements. In the plot 6,
344 this fact is reflected by the elevated value of nugget variance, which is 88% of the sill
345 variance. It could mean that there is a source of spatial variation with a range much smaller
346 than the smallest sampling interval (1 m). This random pattern is probably related to the

347 repeated changes in wind direction observed during the course of fire in plot 6. Increasing the
348 detail of sampling will reveal structure in the apparently random effect of the nugget variance
349 (Burrough, 1983; Webster, 1985).

350 The nugget semivariance, expressed as a percentage of the total semivariance, enables
351 comparison of the relative size of the nugget effect among the studied variable (Trangmar et
352 al., 1985). To define distinct classes of spatial dependence among temperature in the plots,
353 ratios similar to those represented by Cambardella et al. (1994) were used. If the ratio is
354 <25%, the variable is considered strongly spatially dependent; if the ratio is between 25 and
355 75%, the variable is considered moderately spatially dependent; and, if the ratio is >75% the
356 variable is considered weakly spatially dependent. Semivariograms parameters indicated a
357 strong spatial dependence only for soil temperature in plot 8. In plots 1, 2, 4 and 7, soil
358 temperature was characterised by semivariograms with nugget/total semivariance ratios
359 between 25 and 75%, which indicates the existence of moderate spatial dependence. Soil
360 temperature in plot 6 may exhibit spatial dependence at scales smaller than those used in this
361 study (1 m).

362 Punctual kriging at 0.1-m intervals was used to produce an estimation of soil
363 temperatures at unsampled locations inside the plots. The results are displayed as contour
364 maps (Figures 8 - 12). As we choose punctual kriging, which is an exact interpolator in the
365 sense that at the sampling point kriging returns the data, and as the semivariograms in all
366 cases have a nugget variance, the maps show small discontinuities in the kriged surface.

367 Six contour levels are specified for temperature values in high fire severity plots
368 (treatment F2), from $T < 150\text{ }^{\circ}\text{C}$ up to $T > 600\text{ }^{\circ}\text{C}$, with an interval of $75\text{ }^{\circ}\text{C}$. These three plots
369 (plot 1, 4 and 8) showed $T < 300\text{ }^{\circ}\text{C}$ in their lower area, where the fire started. Plot 1 showed a
370 temperature distribution in concentric shape areas (Figure 8). We observed that there are two
371 areas with the highest temperature values (525°C), that coincided with the highest natural

372 biomass points (without taking into account the added biomass). Plot 4 shows the highest
373 values of soil temperature from 10 m to 16 m of their abscissa (Figure 9). In this case, the
374 areas that reached 450 °C and 525 °C covered a higher percentage of plot surface than in plot
375 1. The spatial pattern of soil temperature observed in plots 1 and 4, and those of their pre-fire
376 natural biomass distribution were similar (Figures 8 and 9). In both of them, as we mentioned
377 above, the spatial distribution of the natural vegetation and litter seems to control the
378 temperature patches.

379 However, plot 8 shows clearly a linear pattern of temperature distribution that
380 coincides with the pattern of fire progression (Figures 2 and 10). Temperatures lower than
381 300°C are located in the lower part of the plot and, as the same time as fire front spread, the
382 temperature rises to values higher than 600°C at the upper part of the plot.

383 The contour maps of plots burned with 2 kg m⁻² of additional biomass show
384 temperatures ranging between T<150°C and T>400 °C. Temperatures smaller than 250 °C are
385 distributed over a great part of plot 2, covering two thirds of its total area (Figure 11). At the
386 upper part of this plot, an increase of soil temperatures could be observed, reaching values
387 higher than 350°C. It shows the linear pattern of temperature distribution mentioned above.

388 The contour map of plot 7 (Figure 12) shows that most values are in the range of 150 -
389 250°C, and only two small areas showed temperatures greater than 300°C. The highest values
390 were not found at the upper part of the plot, as occurs when a linear pattern dominates, but
391 temperatures greater than 250°C are found over areas where there was more natural biomass,
392 and where the time of flame persistence was longer.

393 The results obtained suggest that the spatial patterns of soil temperatures during the
394 experimental fires are influenced by the spatial distribution of the natural vegetation. The
395 addition of the extra-biomass contributes to increase the temperatures as well as their
396 residence time on soil surface, but its influence on soil temperature is only evident when the

397 meteorological conditions varies during the course of the fire, especially wind speed and wind
398 direction.

399

400 *3.4. Changes in soil properties induced by fire*

401

402 It is known that the distribution of vegetation in a patchy shrub mosaic, like in this
403 Mediterranean semiarid environment, is related with the spatial and temporal heterogeneity of
404 soil resources, mainly nutrients and water (Schlesinger et al., 1990). On La Concordia plots,
405 as previously studied (Gimeno-García et al., 2001), the presence of shrubs had a clear
406 influence on the dynamics of soil mineral nitrogen, available phosphorus and organic matter,
407 generating a more favourable environment for the enhancement and maintenance of those
408 nutrients than in adjoining bare areas, being a key factor on soil heterogeneity.

409 This vegetation distribution, which play an important role in the soil physical,
410 chemical, hydrological and biological properties, also influence the spatial pattern of
411 temperatures during fire, as has been observed in the present experiment. Soil surface
412 temperatures affect soil properties (Díaz-Fierros et al., 1990; Giovannini et al., 1990; Gimeno-
413 García et al., 2000). Moreover, part of the nutrients accumulated in aboveground biomass and
414 litter are deposited as ash, which contain different amounts of available nutrients in function
415 of the fire severity (Marion et al., 1991; Grogan et al., 2000; Gimeno-García et al., 2000). The
416 spatial patterns of soil temperatures during the studied experimental fires could affect soil
417 properties in a different way, contributing to create a new spatial pattern of soil nutrients. The
418 study of the spatial patterns of those changes is out of the scope of the present paper, but,
419 undoubtedly, they will play an important role in the recovery of the vegetation in burned
420 areas.

421 Generally, the changes on soil properties did not show a linear relationship with the
422 temperature increase during a fire. As Giovannini (1994) stated, these changes in soil
423 properties really respond to the temperature according to a 'discrete step' model. The most
424 important changes occur at different temperature thresholds: temperatures up to 220°C, from
425 220 to 460°C, from 460 to 600°C and beyond 600°C.

426 In the La Concordia soil, there are significant changes in soil chemical properties
427 according to the fire treatment. In plots burned with a moderate intensity (average temperature
428 at the soil sampling points was 222.5°C), soil organic matter and total nitrogen contents
429 increases after the fire by 809 and 7.6 g m⁻², respectively, in the first 5 soil centimetres.
430 However, in plots burned with high intensity (average temperature at the soil sampling points
431 was 466°C), there is a decrease in organic matter and total nitrogen by 94.2 and 5.8 g m⁻²,
432 respectively. Other important changes in soil properties are reported in Table 7, like the
433 increment in available phosphorous, ammonium nitrogen and the exchangeable cations Na, K
434 and Mg, which are proportionally related to the fire severity. However, a decrease of nitrate
435 nitrogen and exchangeable Ca is found in burned soil that is also related to fire severity.

436 The volumetric heat capacity of soil (Cv) calculated before the fire was 0.82 KJ m⁻³ K⁻¹
437 ¹ for dry soil conditions, 1.24 KJ m⁻³ K⁻¹ when the water content at the time of sampling is
438 considered and 2.91 KJ m⁻³ K⁻¹ for soil at field capacity. As consequence of the changes
439 promoted by fire severity on soil organic matter content and soil bulk density, the estimated
440 Cv shows some variation (Figure 13). Cv increases in moderate severity plots for the three-
441 soil water content considered and this increment is related with the rise in soil organic matter
442 content as well as soil bulk density. For high fire severity, there is a slight decrease in the Cv
443 when soil is dry and when the soil water content at the time of sampling is considered,
444 whereas it shows an increase when Cv is calculated for soil at field capacity.

445 As a result of the modifications promoted by fire severity on soil properties, it could
446 be expected a soil nutrient redistribution related to the soil temperature patterns observed,
447 which may be a major factor contributing to heterogeneity in soil nutrient availability and
448 hence to shrub patchiness in this Mediterranean ecosystem. A more detailed study is needed
449 to relate the spatial patterns of soil temperature at the time of burning and the changes in the
450 spatial patterns of soil properties.

451

452

453 **4. Conclusions**

454

455 In the experimental fires carried out in this study, the mean values of soil temperature
456 for each fire treatment were clearly different, but large variations from point to point in soil
457 surface temperatures were observed. In spite of the addition of extra biomass, which
458 contributes to the fire-front spread and continuity, the aboveground vegetation and litter
459 biomass have marked effects in the soil temperature patterns. Moreover, wind speed and
460 direction, and other characteristics of the biomass (both natural and added) as type,
461 compaction and moisture content seems to play also an important role in the spatial
462 distribution of soil temperatures.

463 We observed that soil surface temperature distribution at the burned plots in La
464 Concordia has a moderate spatial dependence when its measurement was made at 1-m
465 interval. Two dominant spatial patterns of temperature distribution in the plots were
466 determined, the spherical model and the linear pattern. The first one varied, in our case,
467 approximately between 4 and 10 m. This pattern is related mainly to the natural biomass
468 distribution and the time of flame persistence.

469 Temperatures increased linearly from the lower to the upper part of the plot, and seem
470 to be controlled by the meteorological conditions at the time of burning, mainly by the wind
471 speed and wind direction. Both patterns of soil temperature distribution are independent of the
472 fire treatment.

473 From the different methods used to assess the temperatures during fire, thermosensitive
474 paints on 1 x 1 m grids, together with the punctual use of thermocouples, have been
475 demonstrated to be a useful tool for characterising the spatial pattern of soil temperatures in
476 five of the six burned plots.

477 The two spatial patterns of soil temperature could play an important role in explaining
478 the changes of soil properties after the fire (physical, chemical and biological), and especially
479 in the spatial distribution of soil nutrients. Fire caused the losses of organic matter, total N,
480 nitrate N and exchangeable calcium in the most severe case. On the other hand, an increase of
481 ammonium N, available phosphorous and Na^+ , K^+ and Mg^{2+} has been quantified, whereas the
482 nitrate N content, the CEC and the exchangeable Ca^{2+} decrease after both severe and
483 moderate fire. Consequently, these changes can affect the distribution and recovery of
484 vegetation in this semiarid ecosystem that has been affected by fire because of plant
485 competition for soil resources.

486

487

488 **Acknowledgements**

489

490 We thank Mr. J. A. Pascual for his assistance with the temperature distribution graphs
491 and D. Rius and E. Barrachina for the soil analysis. We acknowledge support by the EU
492 project 'Postfire soil and vegetation dynamics in natural and afforested areas in Southern
493 Europe: The role of fire intensity' (EV5U-91-0017) for funding this research.

494 **References**

495

496 Black, C.A., Evans, D.D., White, J.L., Ensminger, L.E. and Clark, F.F., 1965. Methods of
497 Soil Analysis: Part 2, Chemical and Microbiological Properties. American Society of
498 Agronomy, Madison, WI.

499 Blake, G. R. and Hartage, K.H., 1986a. Bulk density. In: A. Klute (Editor), Methods of soil
500 analysis, Part 1. American Society of Agronomy, Masiosn, WI, pp. 1364-1367.

501 Blake, G. R. and Hartage, K.H., 1986b. Particle density. In: A. Klute (Editor), Methods of
502 Soil Analysis, Part 1. American Society of Agronomy, Masiosn, WI, pp. 378-379.

503 Bower, C.A., Reitemeir, R.F. and Fireman, M., 1952. Exchangeable cations analysis of saline
504 and alkali soils. *Soil Sci.*, 73: 251-261.

505 Burrough, P.A., 1983. Multiscale sources of spatial variation in soil. I. The application of
506 fractal concepts to nested levels of soil variation. *J. Soil Sci.*, 34: 577-597.

507 Cambardella, C., Moorman, T.B., Novak, J.M., Parkin, T.B. and Karlen, D.L., 1994. Field-
508 Scale Variability of Soil properties in Central Iowa Soils. *Soil Sci. Soc. Am. J.*, 58: 1501-
509 1511.

510 DeBano, L.F. and Conrad, C.E., 1978. The effect of fire on nutrients in a chaparral
511 ecosystem. *Ecology*, 59: 489-497.

512 DeBano, L.F., Neary, D.G. and Ffolliot, P.F., 1998. Fire effects on ecosystems. John Wiley &
513 Sons, New York.

514 Delhomme, J.P., 1978. Kriging in the hydrosociences. *Adv. Water Resour.* 1: 251-266.

515 Demolon, A., 1965. Dinámica del suelo. Omega, Barcelona (in Spanish).

516 Díaz-Fierros, F., Benito, E., Vega, J.A., Castelao, A., Soto, B., Pérez, R and Taboada, T.,
517 1990. Solute loss and soil erosion in burned soil from Galicia (NW Spain). In: J.G.

518 Goldamer and M.J. Jenkins (Editors), *Fire in Ecosystem Dynamics: Mediterranean and*
519 *Northern Perspective*. SPB Academic Publishing. The Hague, pp.103-116.

520 Douchafour, P.H., 1965. *Precís de pedologie*. Masson et Cie, Paris (in French).

521 Etiene, M., 1989. Non destructive methods for evaluating shrub biomass: a review. *Acta*
522 *Oecologica-Oecologia Applicata* 10: 115-128.

523 Etiene, M. and Legrand, C., 1994. A non-destructive method to estimate shrubland biomass
524 and combustibility. *Proceedings 2nd International Conference on Forest Fire Research*, Vol.
525 I, D.X. Viegas, Coimbra, Portugal, pp. 425-434.

526 FAO-UESCO. 1988. *Soil Map of the World. Revised legend. 1: 5.000.000*. FAO, Rome.

527 Gimeno-García, E., Andreu, V. and Rubio, J.L., 2000. Changes in organic matter, nitrogen,
528 phosphorus and cations as a result of fire and water erosion in a Mediterranean landscape.
529 *Eur. J. Soil Sci.*, 51: 201-210.

530 Gimeno-García, E., Andreu, V. and Rubio, J.L.. 2001. Influence of Mediterranean shrub
531 species on soil chemical properties in a typical Mediterranean environment. *Comm. Soil*
532 *Sci. Plant Anal.*, 32 (11-12): 1885-1898.

533 Giovannini, G., 1994. The effect of fire on soil quality. In: M. Sala and J.L. Rubio (Editors),
534 *Soil erosion and degradation as a consequence of forest fire*. Geofoma Ediciones.
535 Logroño, pp 15-27.

536 Giovannini, G., Lucchesi, S. and Giachetti, M., 1990. Effect of heating on some chemical
537 parameters related to soil fertility and plant growth. *Soil Sci.*, 149: 344-350.

538 Grogan, P., Bruns, T.D. and Chapin, F.S., 2000. Fire effects on ecosystem nitrogen cycling in
539 a California bishop pine forest. *Oecologia*, 122: 537-544.

540 Harford, R.A. and Frandsen, W. H., 1992. When it's hot, it's hot-or maybe it's not (surface
541 flaming may not portend extensive soil heating). *Int. J. Wildland Fire*, 2: 139-144.

542 Hillel, D., 1980. *Fundamentals of Soil Physics*. Academic Press, Inc. San Diego, California.

543 Jackson, M.L., 1958. Soil Chemical Analysis. Prentice-Hall, Englewood Cliffs, NJ.

544 Journel, A.G. and Huijbregts, C.J., 1978. Mining geostatistics. Academic Press, London.

545 Marion, G.M., Moreno, J.M. and Oechel, W.C., 1991. Fire severity, ash deposition and
546 clipping effects on soil nutrients in Chaparral. Soil Sci. Soc. Am. J., 55: 235-240.

547 Martínez-Fernández, J., López Bermúdez, F., Romero Díaz, M.A., Alonso Sarriá, F.,
548 Espinosa, V. and Javaloy, A., 1991. El matorral semiárido del sureste de España.
549 Aportación metodológica para su evaluación. Studia Oecologica VIII: 97-105.

550 Ministerio de Agricultura, Pesca y Alimentación, 1986. Métodos Oficiales de Análisis. Tomo
551 III. Secretaría General Técnica, Dirección General de Política Alimentaria, M.A.P.A.,
552 Madrid. (in Spanish).

553 Moreno, J.M. and Oechel, W.C., 1992. Factors controlling post-fire seedling establishment in
554 southern California chaparral. Oecologia, 90: 50-60.

555 Moreno, J.M. and Oechel, W.C., 1994. Fire intensity as a determinant factor of postfire plant
556 recovery in southern California chaparral. In: J.M. Moreno and W.C. Oechel (Editors), The
557 Role of Fire in Mediterranean-Type Ecosystems, Ecological Studies, 107. Springer-Verlag.
558 New York, pp. 26-45.

559 Neary, D.G., Klopatek, C.C., DeBano, L.F. and Ffolliott, P.F., 1999. Fire effects on
560 belowground sustainability: a review and synthesis. Forest Ecol. Management, 122: 51-71.

561 Pérez, B. and Moreno, J.M., 1998. Methods for quantifying fire severity in shrubland-fires.
562 Plant Ecology, 139: 91-101.

563 Primo, E. and Carrasco, J.M., 1973. Química Agrícola I: Suelos y Fertilizantes. Alhambra,
564 Madrid (in Spanish).

565 Pyne, S.J., Andrews, P.L. and Laven, R.D., 1996. Introduction to Wildland Fire. John Wiley
566 & Sons, New York.

567 Richards, L.A., 1954. Diagnosis and improvement of saline and alkali soils. USDA
568 Agriculture Handbook, No 60.

569 Rivas-Martínez, S, 1981. Etages bioclimatiques, secteurs chronologiques et séries de
570 végétation de l'Espagne Méditerranée. *Ecología Mediterránea*, 8 (1-2): 275-288.

571 Robichaud, P.R., Beyers, J.L. and Neary, D.G., 2000. Evaluating the effectiveness of postfire
572 rehabilitation treatments. Gen. Tech. Rep. RMRS-GTR-63. Fort Collins, USDA Forest
573 Service, Rocky Mountain Research Station.

574 Ryan, K.C. and Noste, N.V., 1983. Evaluating prescribed fires. Proceedings Symposium and
575 workshop on wilderness fire. Gen. Tech. Rep. INT-182. J.E. Lotan, B.M. Kilgore, W.C.
576 Fischer and R.W. Mutch, Ogden, UT, pp.230-238.

577 Schlesinger, W.H., Reynolds, J.F., Cunningham, G.L., Huenneke, L.F., Jarrell, W.M.,
578 Virginia, R.A. and Whitford, W.G., 1990. Biological feedbacks in global desertification.
579 *Sci.* 247: 1043-1048.

580 Trangmar, B.B., Yost, R.S. and Uehara, G., 1985. Application of geostatistics to spatial
581 studies of soil properties. *Advances in Agronomy*, 38: 45-94.

582 Webster, R., 1985. Quantitative Spatial Analysis of Soil in the Field. *Advances in Soil*
583 *Science*, 3: 1-70.

584 Webster, R. and Olivier, M.A., 1990. Statistical Methods in Soil Land Resource Survey.
585 Oxford Univ. Press, New York.

586

587 Table 1
 588 Some soil physical and chemical properties of La Concordia plots
 589

	Horizons		
	Ah1	Ah2	Ck
Depth (cm)	0-12	12-30	30-40
% Sand (2-0.05 mm)	60.84	-	-
% Silt (0.05-0.002 mm)	27.88	-	-
% Clay (< 0.002 mm)	7.52	-	-
Texture	Sandy loam	-	-
Water retention at field capacity (%)	30.83	28.54	29.55
Aggregate stability (%)	32.95	39.70	-
Particle density (g cm ⁻³)	1.87	-	-
Bulk density (g cm ⁻³)	0.74	-	-
Organic matter (%)	9.81	6.22	4.72
pH	7.17	7.30	7.21
Electric conductivity (dS.m ⁻¹)	0.71	0.59	0.99
Total carbonate (%)	43.01	56.72	69.89
Total Nitrogen (%)	0.41	0.29	0.24
Mineral nitrogen (mg kg ⁻¹)	15.67	9.63	17.66
Available phosphorus (mg kg ⁻¹)	3.50	3.30	3.30
CEC (cmol _c . kg ⁻¹)	29.46	29.02	27.28

590

591

592 Table 2

593 Vegetation characteristics of La Concordia: Plant community composition, mean total above-
 594 ground biomass per plot (standing plants and litter), cover percentage in each plot before the
 595 experimental fires and percentage of the dominant species

	Plots					
	1	2	4	6	7	8
Biomass (kg m ⁻²)	0.652	0.702	0.793	0.827	0.443	0.586
Soil cover (%)	20.10	21.58	21.58	23.35	23.01	21.32
Species (%)						
<i>Rosmarinus officinalis</i>	48.29	34.63	40.54	43.29	31.36	9.09
<i>Cistus clusii</i>	2.93	0.98	6.31	0.61	1.78	4.85
<i>Rhamnus lycioides</i>	5.37	3.41	11.71	4.27	1.18	3.03
<i>Ulex parviflorus</i>	28.29	16.10	18.02	20.73	7.69	18.18
<i>Globularia alypum</i>	6.83	40.00	18.92	20.12	47.93	30.91
<i>Thymus vulgaris</i>	1.46	0.49	2.70	4.27	7.69	23.64
<i>Stipa tenacissima</i>	0.49	2.44	-	3.66	-	0.61
<i>Erica multiflora</i>	1.95	-	-	-	-	-
<i>Pinus halepensis</i>	0.49	-	-	0.61	-	0.61
<i>Quercus coccifera</i>	3.90	-	0.90	-	2.37	8.48
<i>Anthyllis cytisoides</i>	-	1.95	0.90	2.44	-	0.61
<i>Brachypodium retusum</i>	+++	+++	+++	+++	+++	+++

596

597 (-) Absent

598 (+++) Frequent

599

600 Table 3

601 Meteorological conditions during experimental fires and fire spread rate

Date	Burned plots	Air temperature (°C)	Relative humidity (%)	Wind rate (m s ⁻¹)	Prevailing wind	Rate of fire front (m s ⁻¹)
20 June 1995	1	21	71	0.3	SE	0.081
	2	22	71	0.3	SE	0.210
	4	20	85	0.3	SE	0.133
21 June 1995	6	24	79	0.3 - 1.4	SE and SW	0.222
	7	22	82	0.3	SE	0.266
	8	22	83	0.3	SE	0.117

602

603 Table 4

604 (a) Average and peak soil temperatures (°C) measured with thermosensitive paints and
 605 thermocouples at the same points (n= 6) in La Concordia plots and (b) results of the ANOVA
 606 test to study statistical differences between the burned plots and between the two methods for
 607 measuring temperatures

608

609 (a)

Fire treatment	Plot	Average T		Peak T	
		Paints	Thermocouples	Paints	Thermocouples
F1 (biomass 2 kg m ⁻²)	2	301.0	347.3	525	440
	6	266.3	381.8	621	633
	7	209.5	- ^a	621	-
F2 (biomass 4 kg m ⁻²)	1	516.6	451.5	677	639
	4	546.8	629.5	677	754
	8	453.5	500.3	677	654

610

611 ^a Thermocouples in plot 7 failed during the experimental fire, so the data are not included

612

613 (b)

Source	Sum of squares	df.	Mean squares	F ratio	Significance
Plot	625079.9	4	156269.9	10.975	0.000
Method measurement	30826.6	1	30826.6	2.165	0.147
Plot x Method	55261.1	4	13815.3	0.970	0.432
Error	711937.0	50	14238.7		

614

615 Table 5

616 Summary statistics for temperature data (°C) measured with the thermosensitive paints

617

Fire treatment	F2 (4 kg m ⁻²)			F1 (2 kg m ⁻²)		
Plot	1	4	8	2	6	7
N	80	80	80	80	80	80
Mean (°C) ^a	417.78 a	448.09 a	434.91 a	239.90 b	239.46 b	217.54 b
Median	420.00	454.00	420.00	226.00	226.00	198.00
Std. deviation ^b	118.78	132.63	147.32	90.71	91.58	81.61
CV (%) ^c	28.43	29.597	33.874	37.81	38.245	37.516
IQR ^d	177.25	200.75	182.00	65.00	65.00	65.00
Mínimum (°C)	226	170	170	101	149	76
Máximum (°C)	677	677	677	525	621	621
Skewness	0.127	-0.030	0.145	1.731	2.186	2.381
Kurtosis	-0.749	-0.717	-0.663	2.824	5.947	8.239
Variance	14108	17589	21705	8227	8387	6661

618

619

620 ^a Different lower case letter among F1 and F2 treatments indicates statistically significant
621 difference at P< 0.05

622 ^b Standard deviation

623 ^c Coefficient of variation

624 ^d Interquartile range

625

626 Table 6

627 Parameters of the geostatistical analysis of soil surface temperature distribution in La Concordia experimental plots

628

Plots		1	2	4	6	7	8
Semivariance parameters	Lag distance maximum	19.235	19.235	19.235	19.235	19.235	19.235
	Lag distance active	11.541	11.541	11.541	11.541	11.541	11.541
	Step size minimum	1	1	1	1	1	1
	Step size active	2	2	2	2	2	2
	N° classes lag	5	5	5	5	5	5
	Pairs of points per class	> 250	> 250	> 250	> 250	> 250	> 250
Semi-variogram	Best fit isotropic model	Spherical	Linear	Spherical	Linear	Spherical	Linear
	R ²	0.788	0.708	0.874	0.199	0.957	0.959
	Nugget variance (c ₀)	7230	4718.2	10700	7808	5000	3952.6
	Sill (c ₀ + c)	14220	8366.7	18190	8893	8547	27537
	Range (a ₀)	3.81	11.541	9.280	11.541	10.29	11.541
	(Nugget /Sill) ^a	50.84 M	56.39 M	58.82 M	87.79 W	58.50 M	14.35 S
Kriging	Type of kriging	Punctual	Punctual	Punctual	Punctual	Punctual	Punctual
	Interval between points	0.1	0.1	0.1	0.1	0.1	0.1
	Size radius	19.235	19.235	19.235	19.235	19.235	19.235
	N° maximum neighbours	8	8	8	8	8	8
Jack-knifing	Reduced error. Mean	0.039	0.030	0.02	0.053	0.024	0.055
	Reduced error. Variance	0.708	0.837	0.708	0.766	0.702	1.030

629

630 ^a Class of spatial dependence. W: weak; M: moderate; S: strong

631

632

633 Table 7

634 Changes of soil properties in La Concordia plots as consequence of fire at the soil sampling
635 points for each fire treatment. Values followed by (+) indicate an increase respect their values
636 before burning and values followed by (-) indicate a decrease respect their values before the
637 fire

638

	Fire severity	
	Moderate	High
Organic matter (g m ⁻²)	809.1 (+)	94.2 (-)
Total Nitrogen (g m ⁻²)	7.6 (+)	5.8 (-)
Ammonium Nitrogen (g m ⁻²)	1.7 (+)	3.0 (+)
Nitrate Nitrogen (g m ⁻²)	0.4 (-)	0.7 (-)
Available Phosphorus (g m ⁻²)	1.2 (+)	2.0 (+)
Na ⁺ (g m ⁻²)	6.1 (+)	5.9 (+)
K ⁺ (g m ⁻²)	7.3 (+)	9.8 (+)
Mg ²⁺ (g m ⁻²)	1.4 (+)	1.4 (+)
Ca ²⁺ (g m ⁻²)	46.5 (-)	55.0 (-)

639

640

641

642 *Figure captions*

643

644 Figure 1. Natural biomass distribution ranges (kg m^{-2}) and their percentages in the La
645 Concordia plots

646

647 Figure 2. Schematic representation of fire progression for the plots of high fire severity (F2).
648 Lines inside the plots indicate the fire progression at different time intervals. The numbers
649 correspond with the time (minutes and seconds) of fire spread across the plots. Arrows
650 indicates the main changes of wind direction

651

652 Figure 3. Schematic representation of fire progression for the plots of moderate fire severity
653 (F1). Lines inside the plots indicate the fire progression at different time intervals. The
654 numbers correspond with the time (minutes and seconds) of fire spread across the plots.
655 Arrows indicates the main changes of wind direction

656

657 Figure 4. Relationship between soil temperature at the soil surface and amount of natural
658 biomass per square metre in the burned plots

659

660 Figure 5. Soil temperature at the soil surface in each burned plot related with the distance
661 covered by the fire line. Zero value from X axis represents the fire start point

662

663 Figure 6. Experimental semivariograms and fitted models for soil temperature in F2 plots. (a)
664 Spherical model for plot 1; (b) Spherical model for plot 4; (c) Lineal model for plot 8.
665 Symbols are the experimental semivariances (γ) and the solid line represents the fitted model

666 Figure 7. Isotropic semivariograms and fitted models for soil temperature in F1 plots. (a)
667 Lineal model for plot 2; (b) Lineal model for plot 6; (c) Spherical model for plot 7. Symbols
668 are the experimental semivariances (γ) and the solid line represents the fitted model

669

670 Figure 8. Map of the kriged estimates for temperature at the soil surface of Plot 1 measured
671 with thermosensitive paints (right) and spatial distribution of natural biomass amount per
672 square metre (left)

673

674 Figure 9. Map of the kriged estimates for temperature at the soil surface of Plot 4 measured
675 with thermosensitive paints (right) and spatial distribution of natural biomass amount per
676 square metre (left)

677

678 Figure 10. Map of the kriged estimates for temperature at the soil surface of Plot 8 measured
679 with thermosensitive paints of Plot 8 (right) and spatial distribution of natural biomass
680 amount per square metre (left)

681

682 Figure 11. Map of the kriged estimates for temperature at the soil surface of Plot 2 measured
683 with thermosensitive paints (right) and spatial distribution of natural biomass amount per
684 square metre (left)

685

686 Figure 12. Map of the kriged estimates for temperature at the soil surface of Plot 7 measured
687 with thermosensitive paints (right) and spatial distribution of natural biomass amount per
688 square metre (left)

689

690 Figure 13. Volumetric heat capacity estimated for three different soil water conditions: (A)
691 dry soil; (B) soil water content at the time of sampling; (C) soil at field capacity. Calculations
692 were made before fire and after fire for the three fire treatments: High fire severity (H),
693 Moderate fire severity (M); Control treatment (C)
694

695
696
697
698
699
700
701
702
703
704
705
706
707
708
709
710
711
712
713
714
715
716
717
718

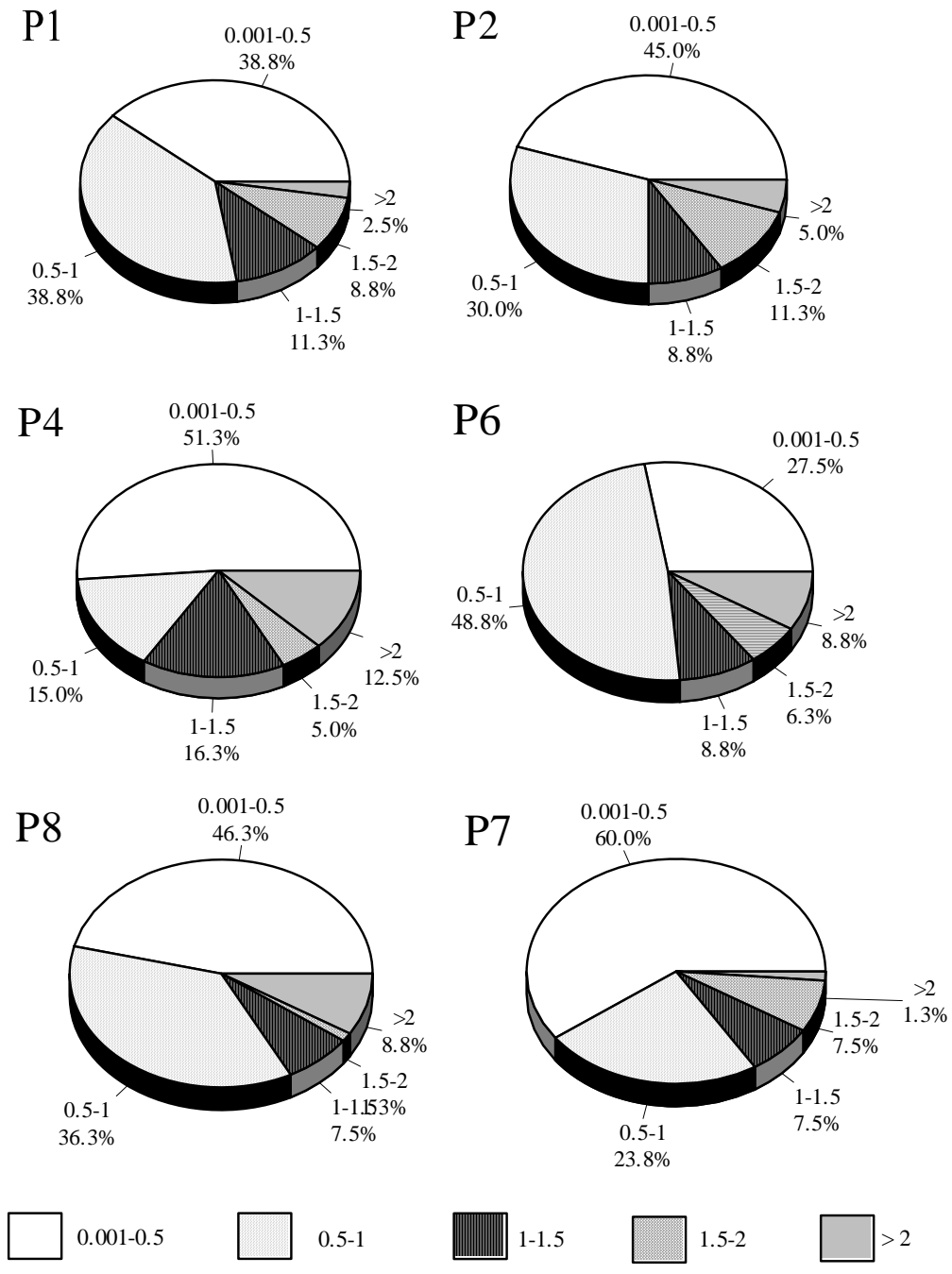


Fig. 1

719
720
721
722
723
724
725
726
727
728
729
730
731
732
733
734
735

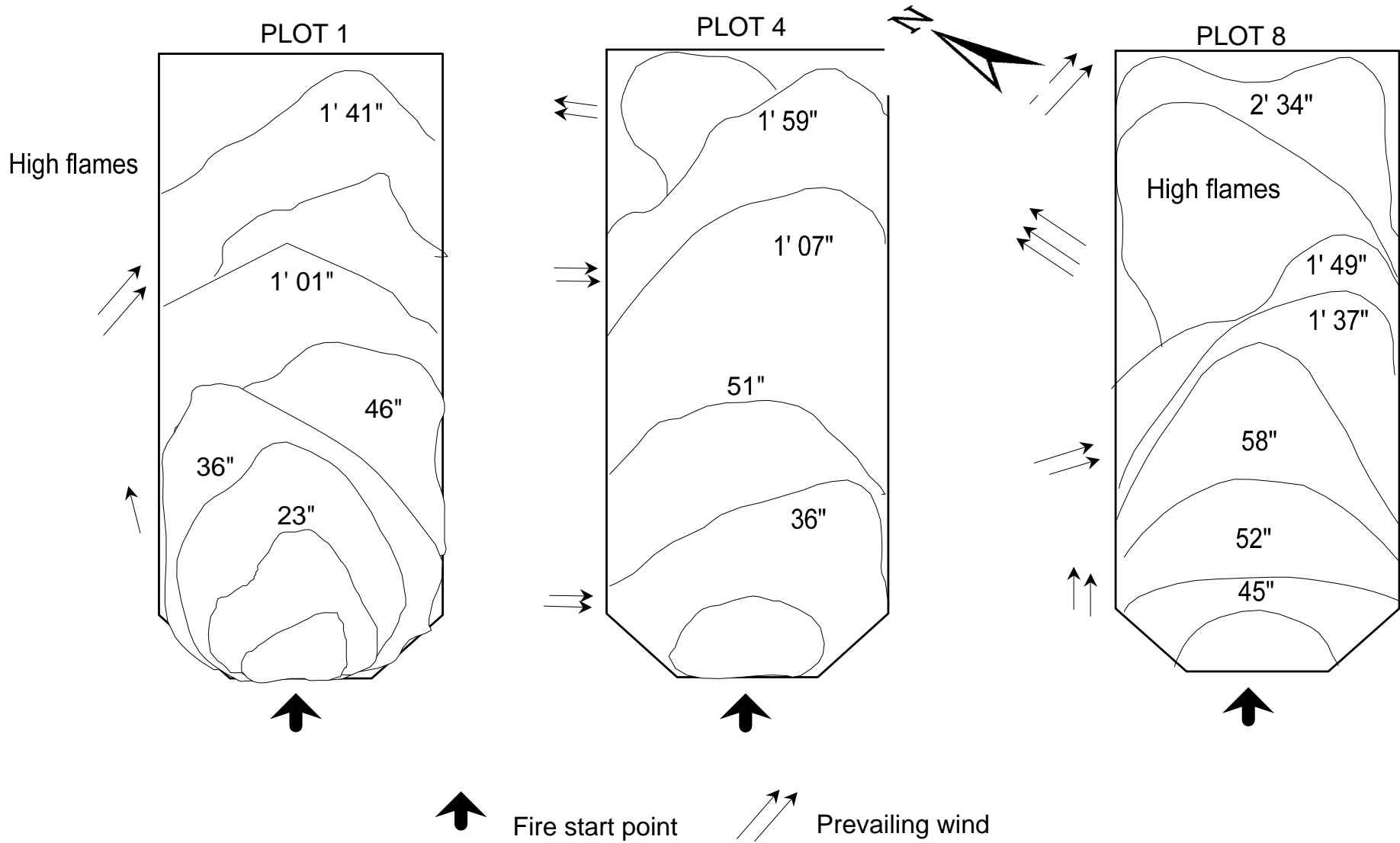


Fig. 2

736
737
738
739
740
741
742
743
744
745
746
747
748
749
750
751

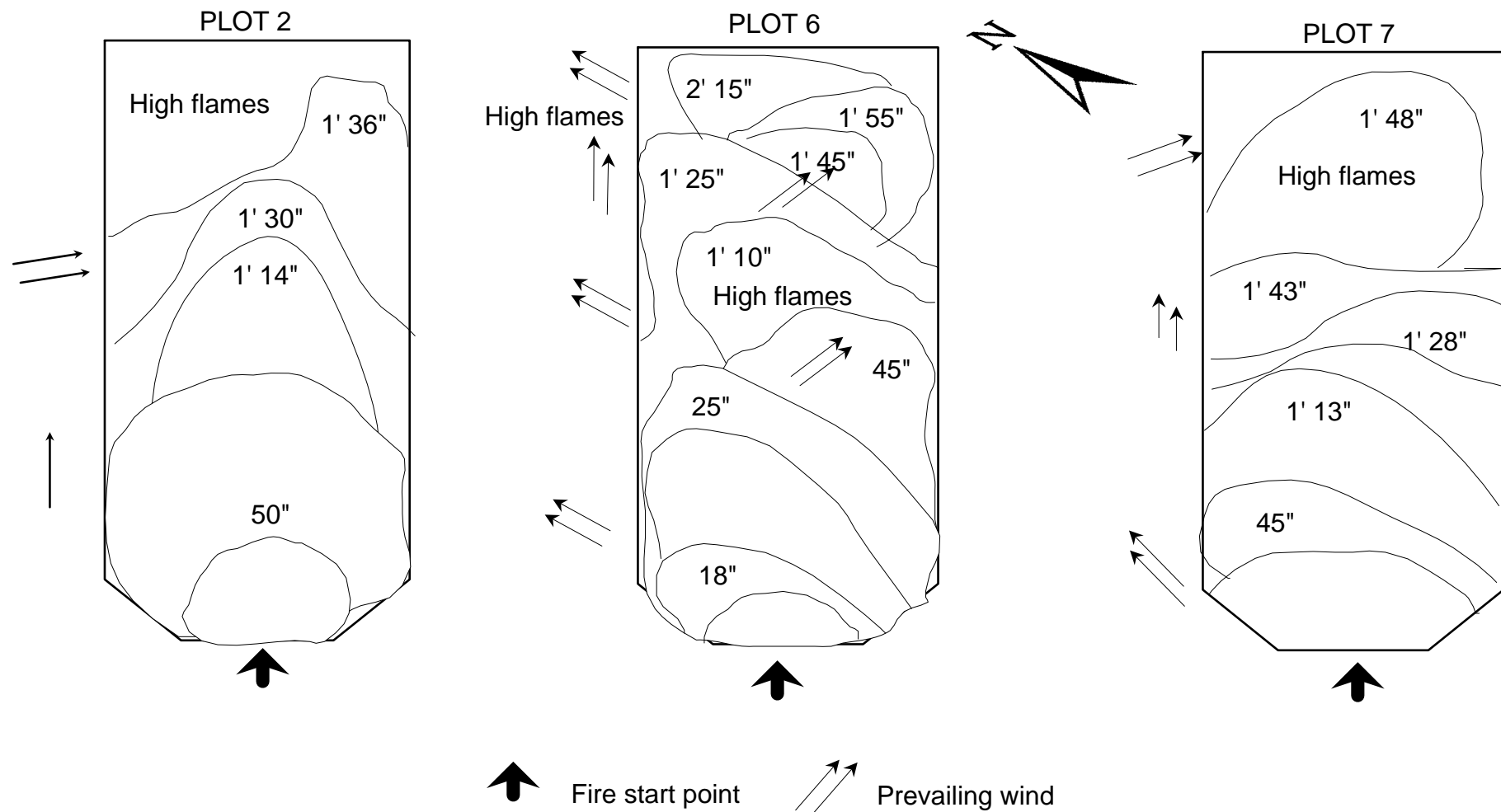
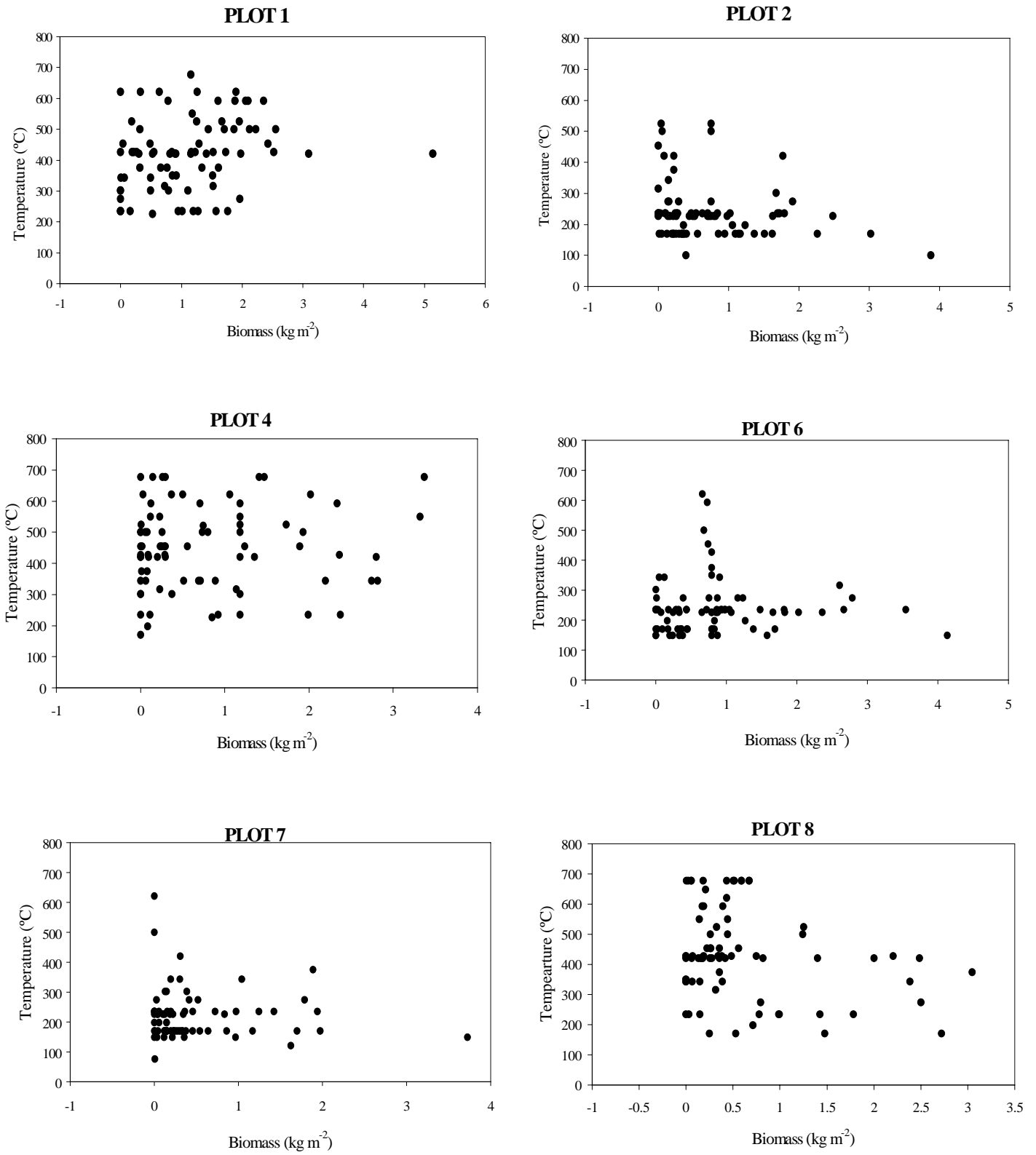
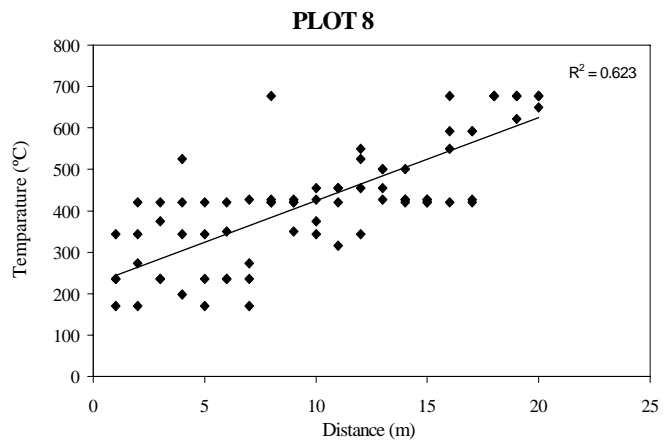
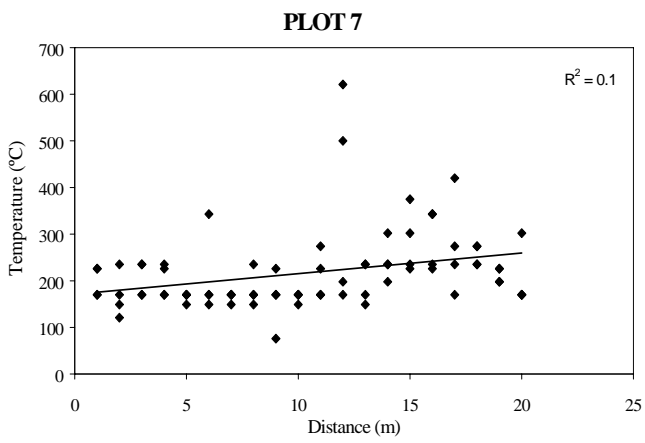
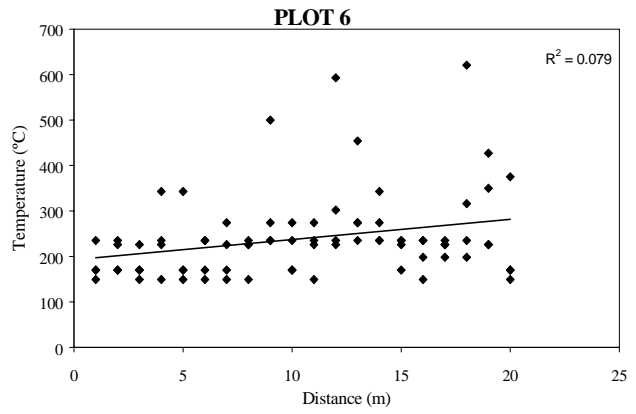
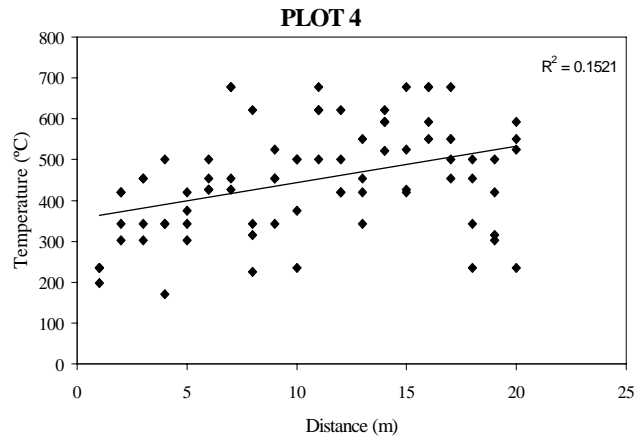
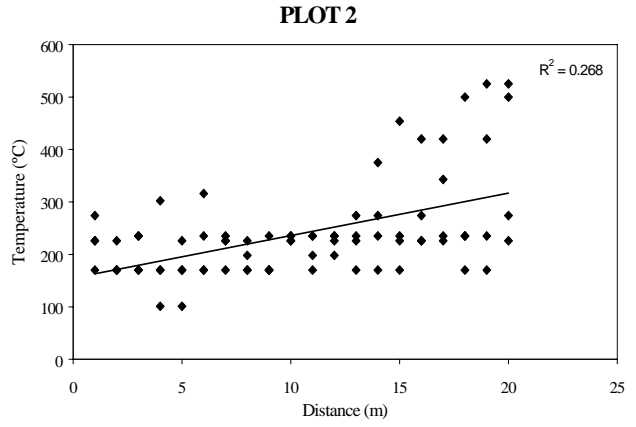
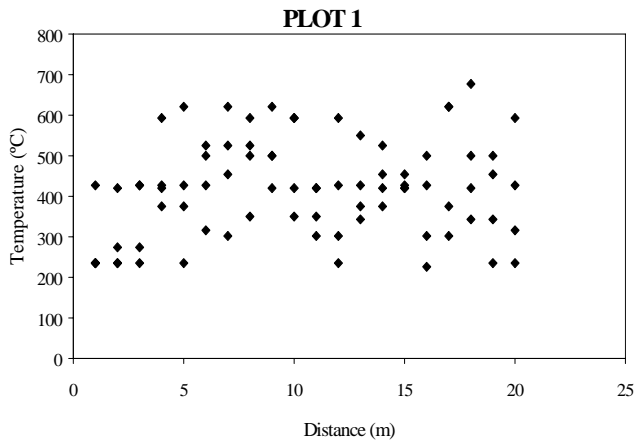


Fig. 3



753 Fig. 4

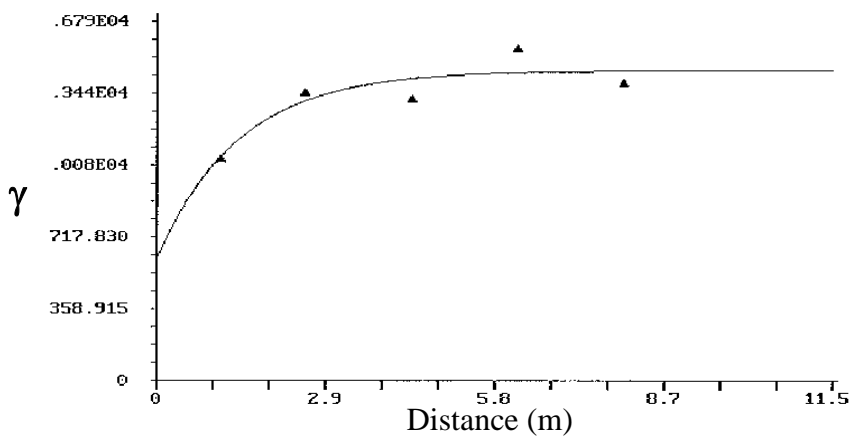


755
756 Fig. 5

757

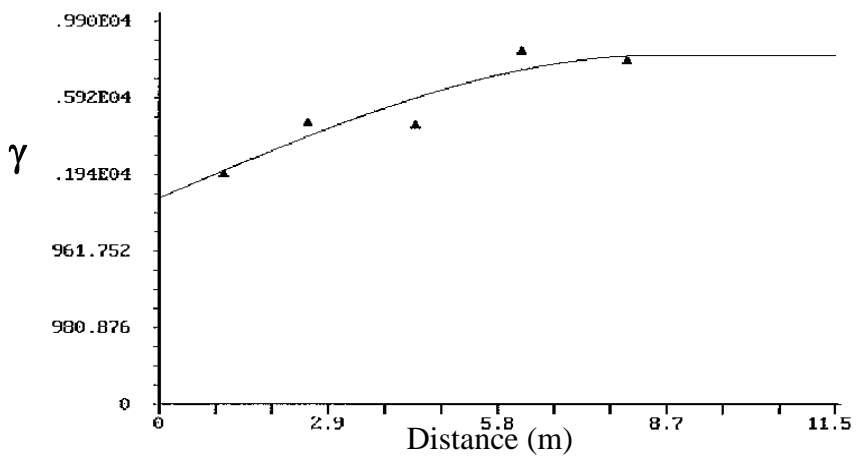
758
759
760
761
762
763
764
765
766
767
768
769
770
771
772

(a) Plot 1



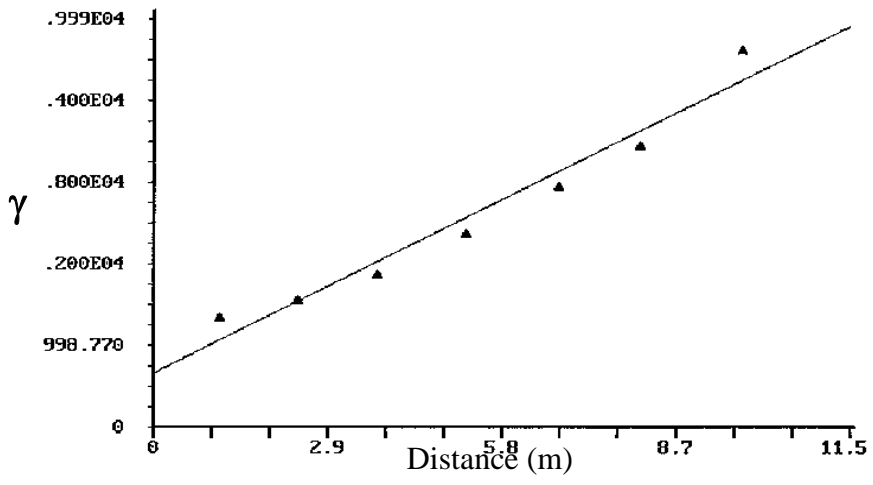
773
774
775
776
777
778
779
780
781
782
783
784
785
786
787
788
789

(b) Plot 4



790
791
792
793
794
795
796
797
798
799
800
801
802
803
804
805
806

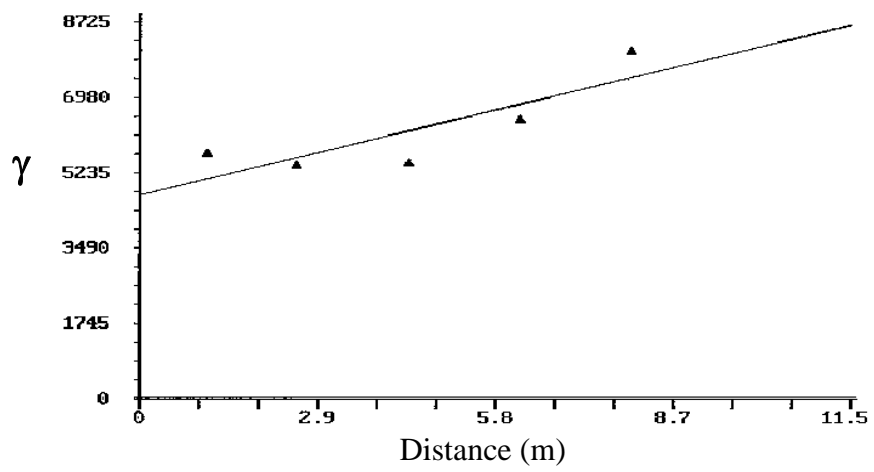
(c) Plot 8



807 Fig. 6
808

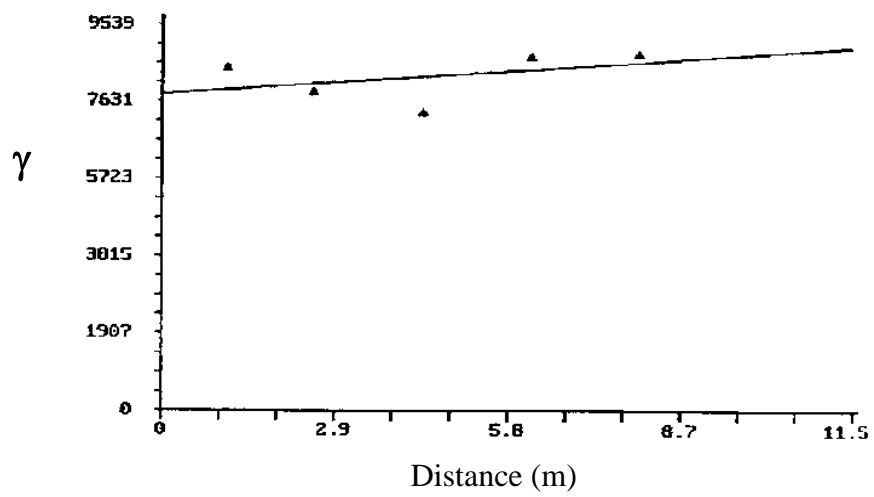
809
810
811
812
813
814
815
816
817
818
819
820
821
822
823
824

(a) Plot 2



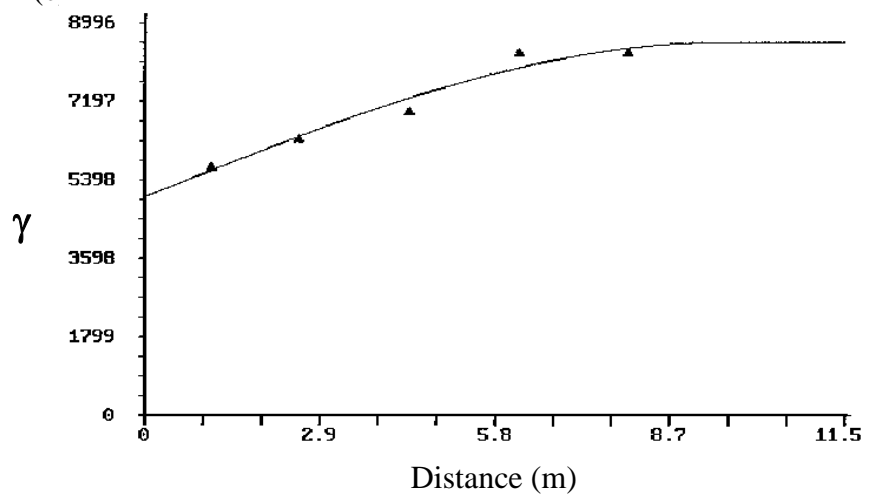
825
826
827
828
829
830
831
832
833
834
835
836
837
838
839
840
841

(b) Plot 6



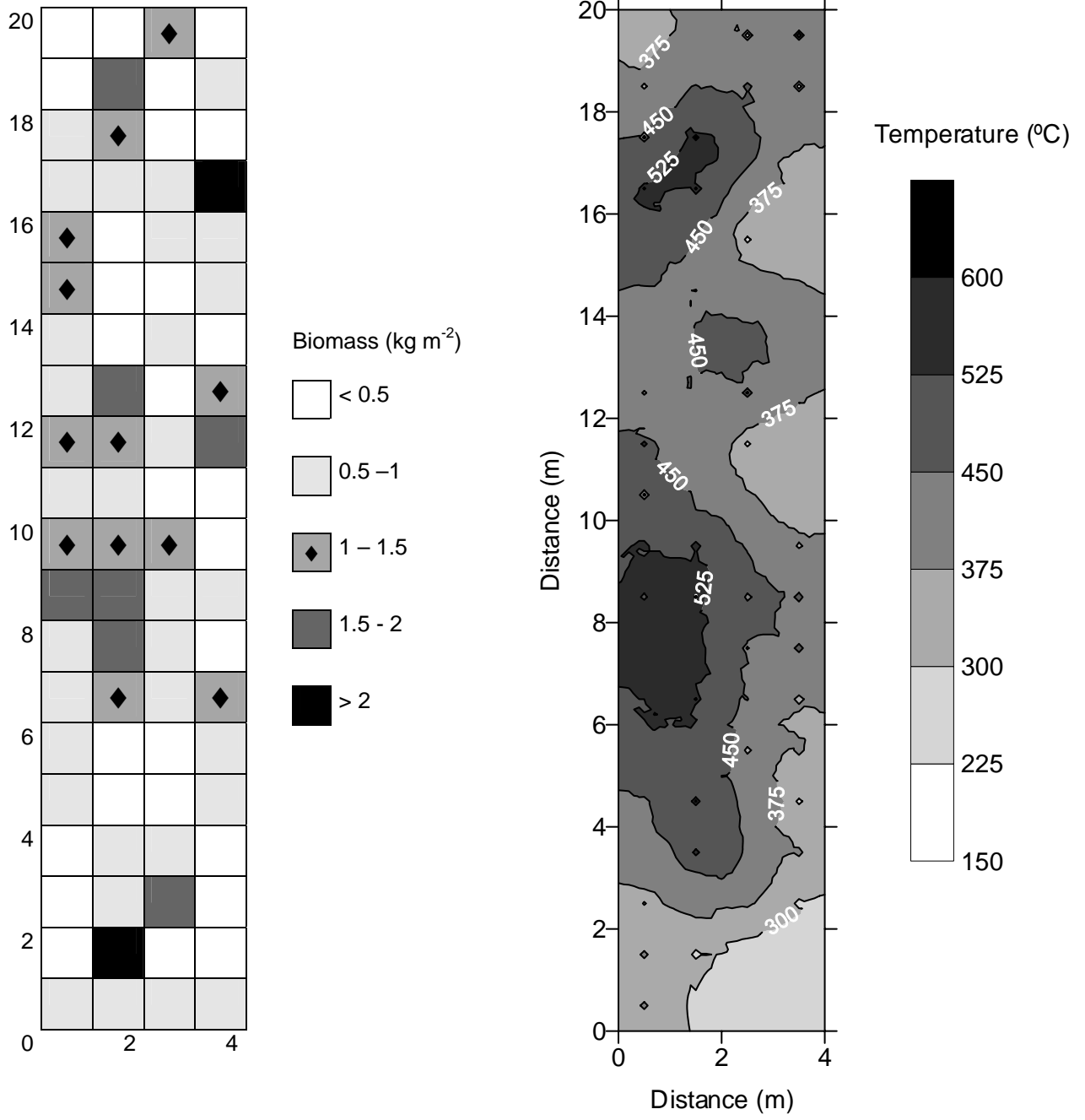
842
843
844
845
846
847
848
849
850
851
852
853
854
855
856
857
858

(c) Plot 7



859 Fig. 7
860

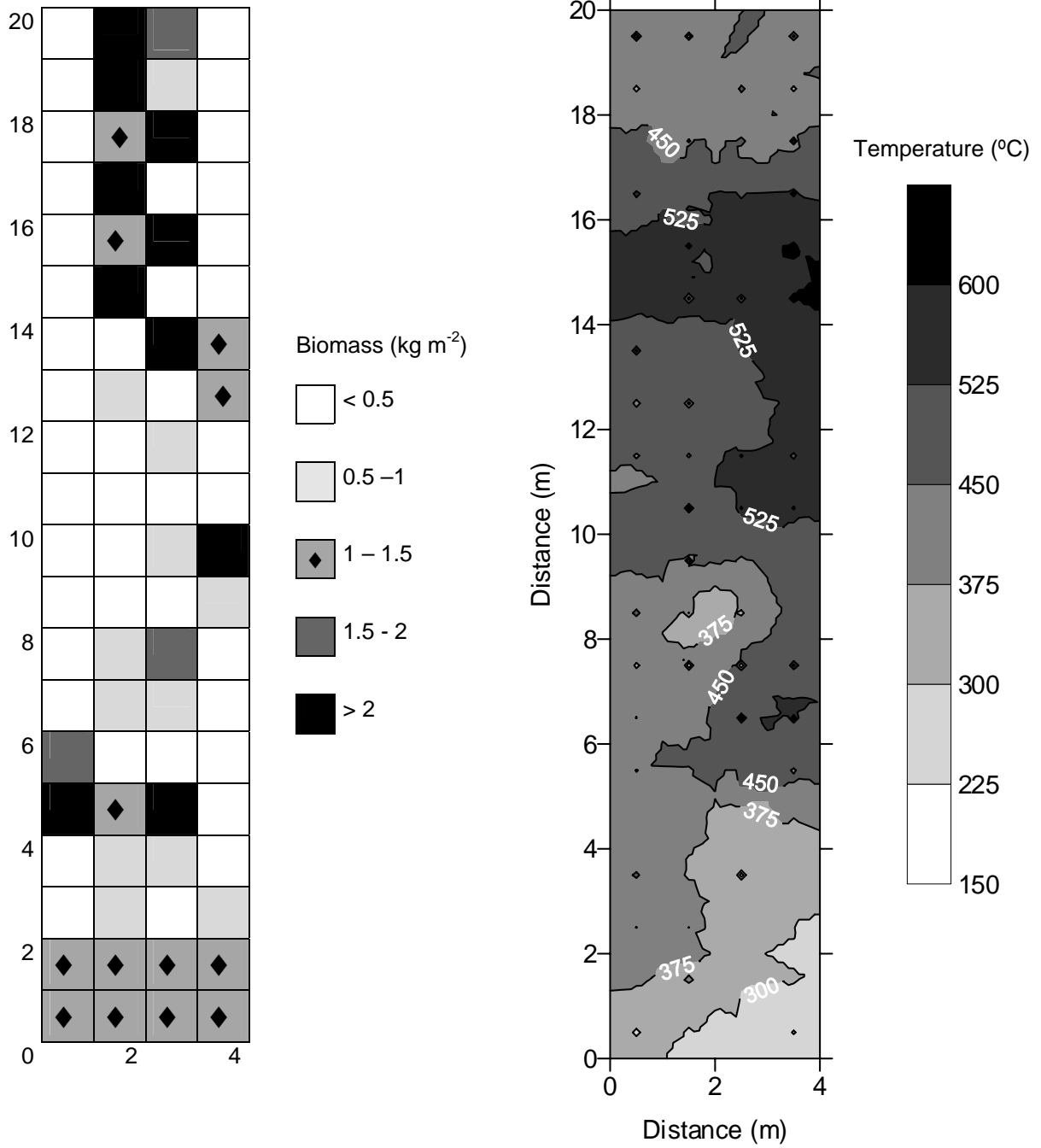
PLOT 1



861
862
863
864
865
866
867

Fig. 8

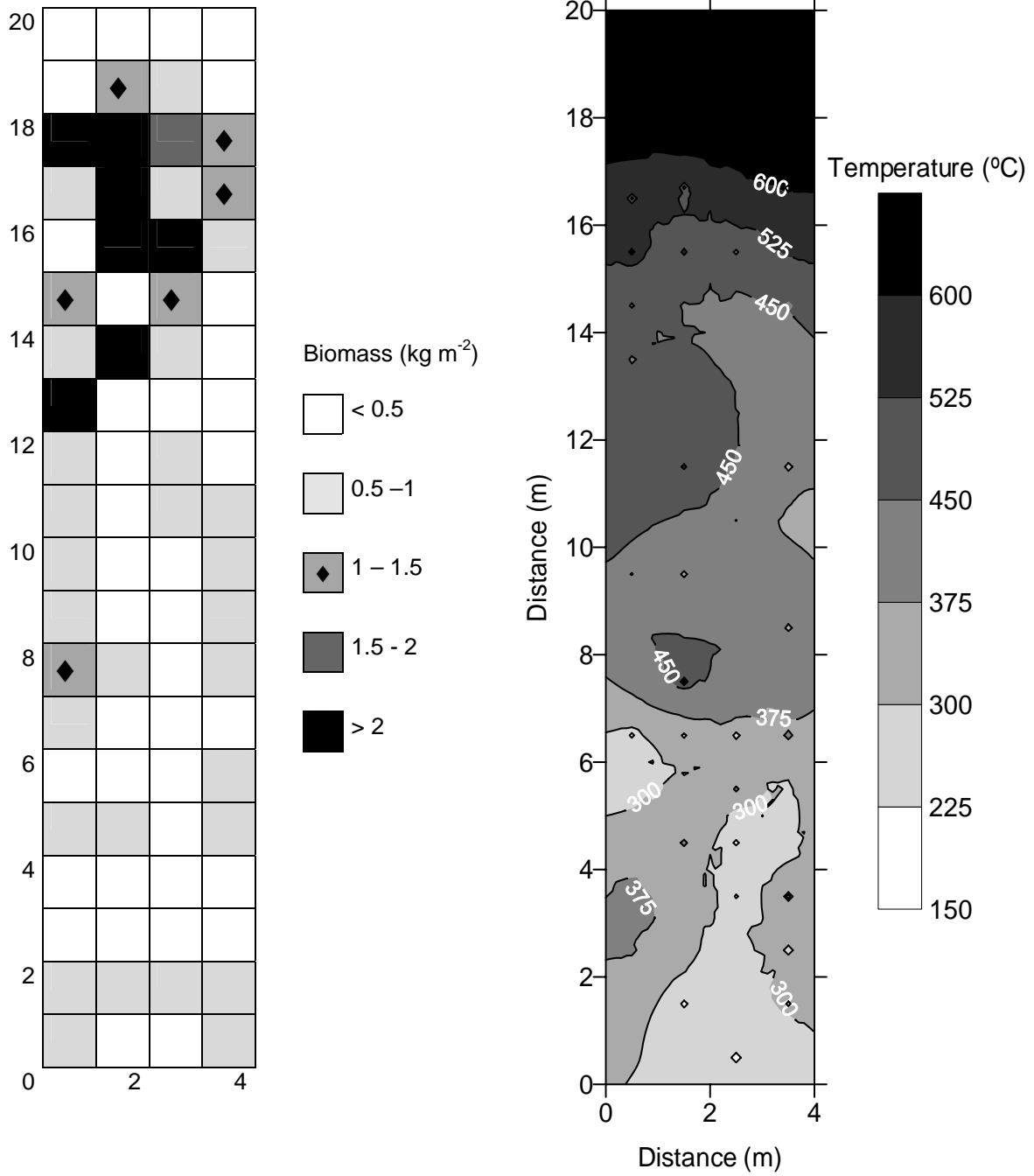
PLOT 4



868
869
870
871
872

Fig. 9

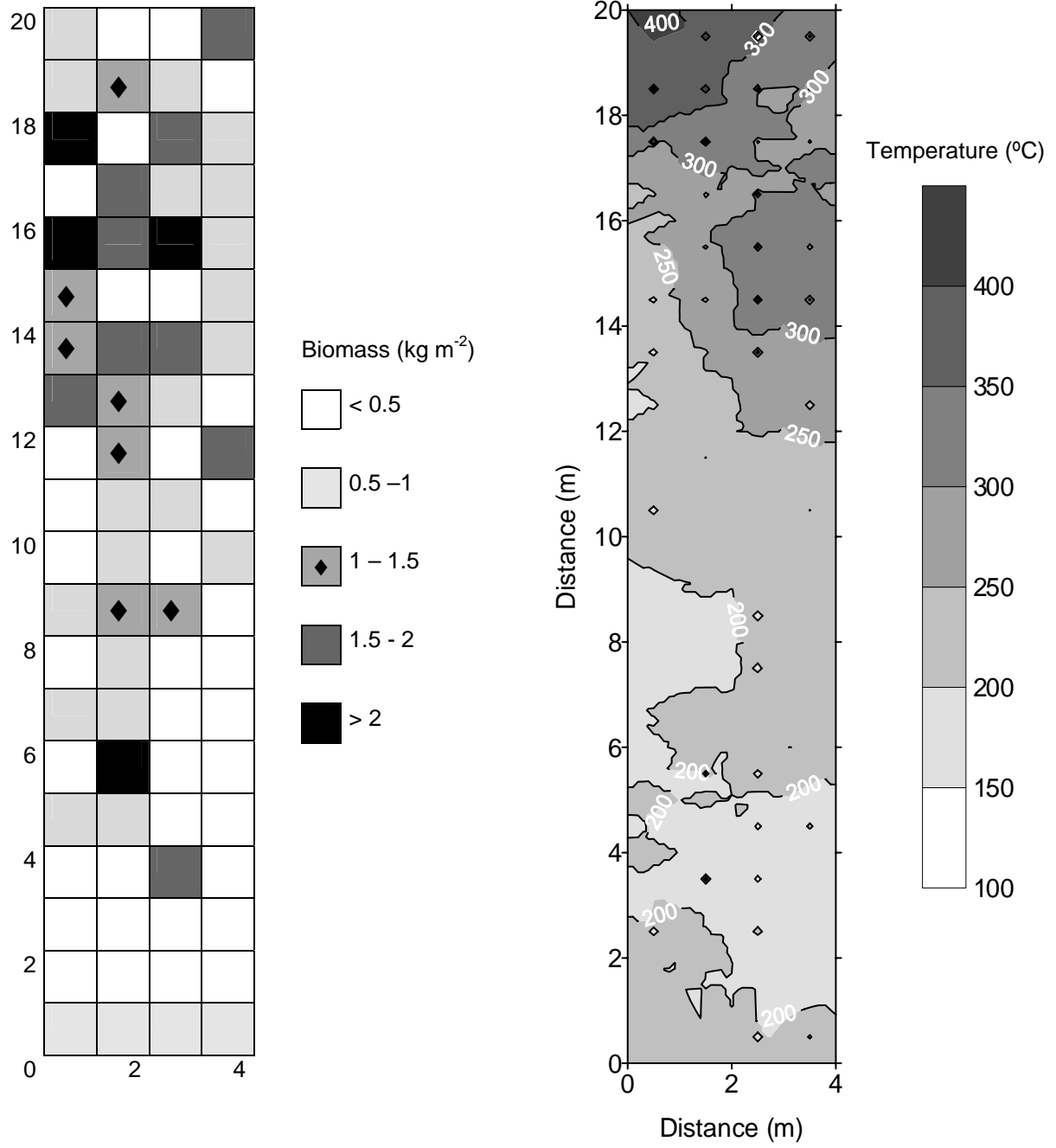
PLOT 8



873
874
875
876
877
878

Fig. 10

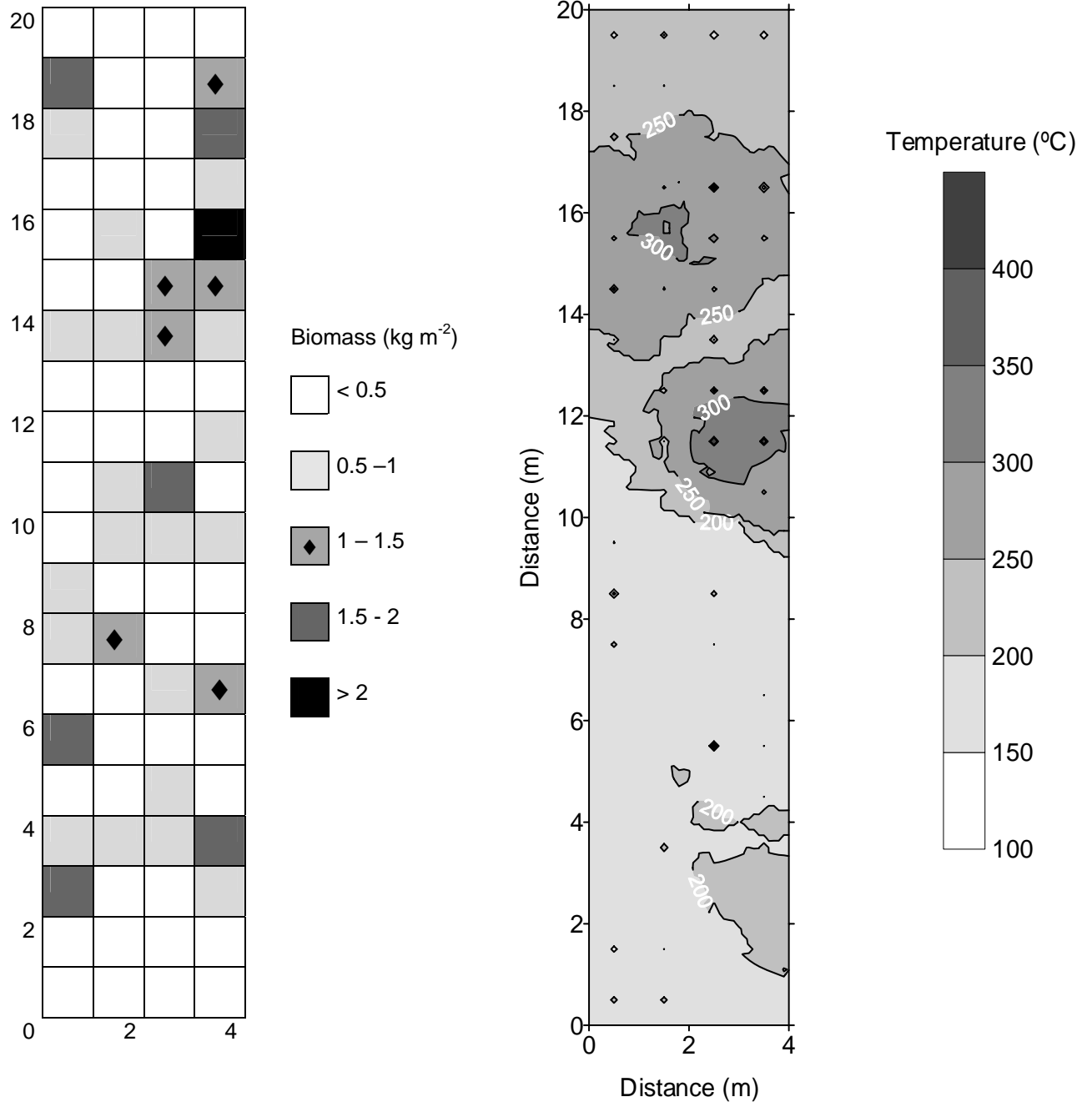
PLOT 2



879
880
881
882
883
884

Fig. 11

PLOT 7

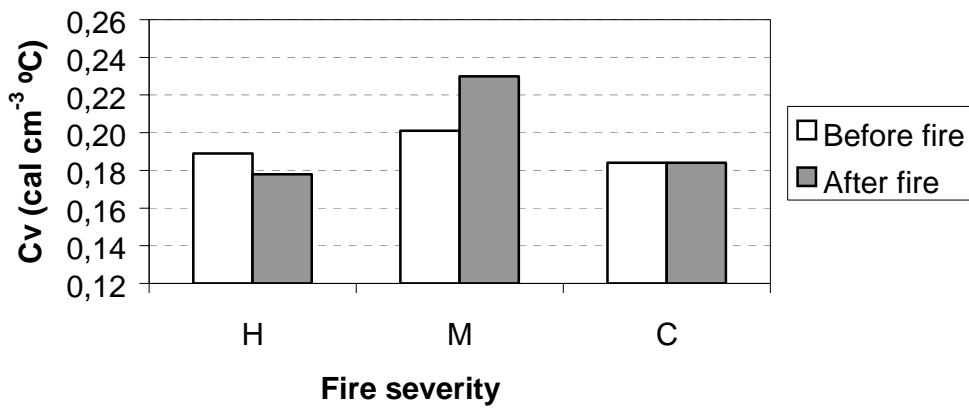


885
886
887
888
889
890
891

Fig. 12

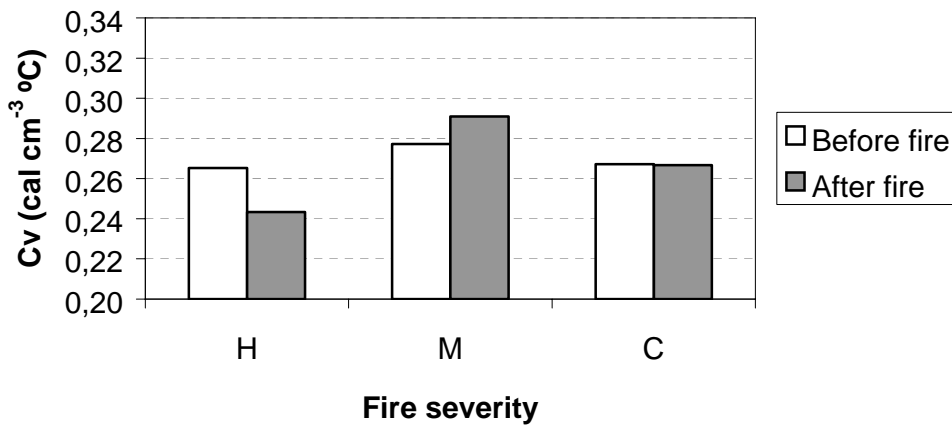
892 A)

Cv dry conditions



910 B)

Cv at time of sampling



931 C)

Cv field capacity

